ELSEVIER

Journal of Quantitative Spectroscopy & Radiative Transfer 109 (2008) 2291–2302

Journal of Quantitative Spectroscopy & Radiative Transfer

www.elsevier.com/locate/jqsrt

Water-vapor continuum absorption in the 800–1250 cm^{-1} spectral region at temperatures from 311 to 363 K

Yu.I. Baranov[a], W.J. Lafferty[a,*], Q. Ma[b,c], R.H. Tipping[d]

[a]*Optical Technology Division, National Institute of Standards and Technology (NIST), Gaithersburg, MD 20899, USA*
[b]*Department of Applied Physics, Columbia University, USA*
[c]*Goddard Space Flight Center, Institute for Space Studies, 2880 Broadway, New York, NY 10025, USA*
[d]*Department of Physics and Astronomy, University of Alabama, Tuscaloosa, AL 35487-0324, USA*

Received 9 November 2007; received in revised form 10 March 2008; accepted 11 March 2008

Abstract

About 200 pure water-vapor spectra covering the region from 800 to 3500 cm^{-1} were recorded with resolution of 0.1 cm^{-1} at temperatures 311, 318, 325, 339, 352, and 363 K using a 2 m base White cell coupled to the BOMEM DA3.002 FTIR spectrometer. The water-vapor pressure varied from 28 to 151 mbar (21–113 Torr). Under these conditions, the continuum absorbance is quite measurable with the available path lengths up to 116 m. A program was developed for spectral processing that calculates, fits, and removes ro-vibrational structure from the spectrum. The spectra obtained were used to retrieve averaged and smoothed binary absorption coefficients over the region from 800 to 1250 cm^{-1}. Our continuum data extrapolated to room temperature are in reasonable agreement with the MT_CKD continuum model. But at higher temperatures the MT_CKD model provides very low values, which are up to 50% less than those experimentally measured. Published by Elsevier Ltd.

Keywords: Water-vapor absorption spectra; MT_CKD continuum; Atmospheric absorption

1. Introduction

The water-vapor continuum absorption in the atmospheric window from 800 to 1250 cm^{-1} strongly affects the Earth's outgoing radiation and therefore is of great importance for radiative budget calculations [1,2]. The history of experimental and theoretical investigations of the water-vapor continuum extends back many decades beginning with the work of Elsasser [3]. In the 1970s these studies were intensified due to progress in laser technology. Application of CO_2 and other gas and diode lasers to environmental research, remote sensing, atmospheric spectroscopy, etc. required a detailed knowledge of the processes affecting laser beam propagation through the atmosphere. Many scientific groups in the world contributed to this investigation from that time using different instrumentation and methods. Nevertheless, the observed data are still incomplete and not precise enough to satisfy present-day requirements. The water-vapor continuum absorption is quite weak, and even very sensitive methods of measurement may lead to large errors. The origin of this absorption is also not clear, and further

*Corresponding author. Tel.: +1 301 975 2375; fax: +1 301 869 5700.
E-mail address: Walter.Lafferty@nist.gov (W.J. Lafferty).

0022-4073/$ - see front matter Published by Elsevier Ltd.
doi:10.1016/j.jqsrt.2008.03.004

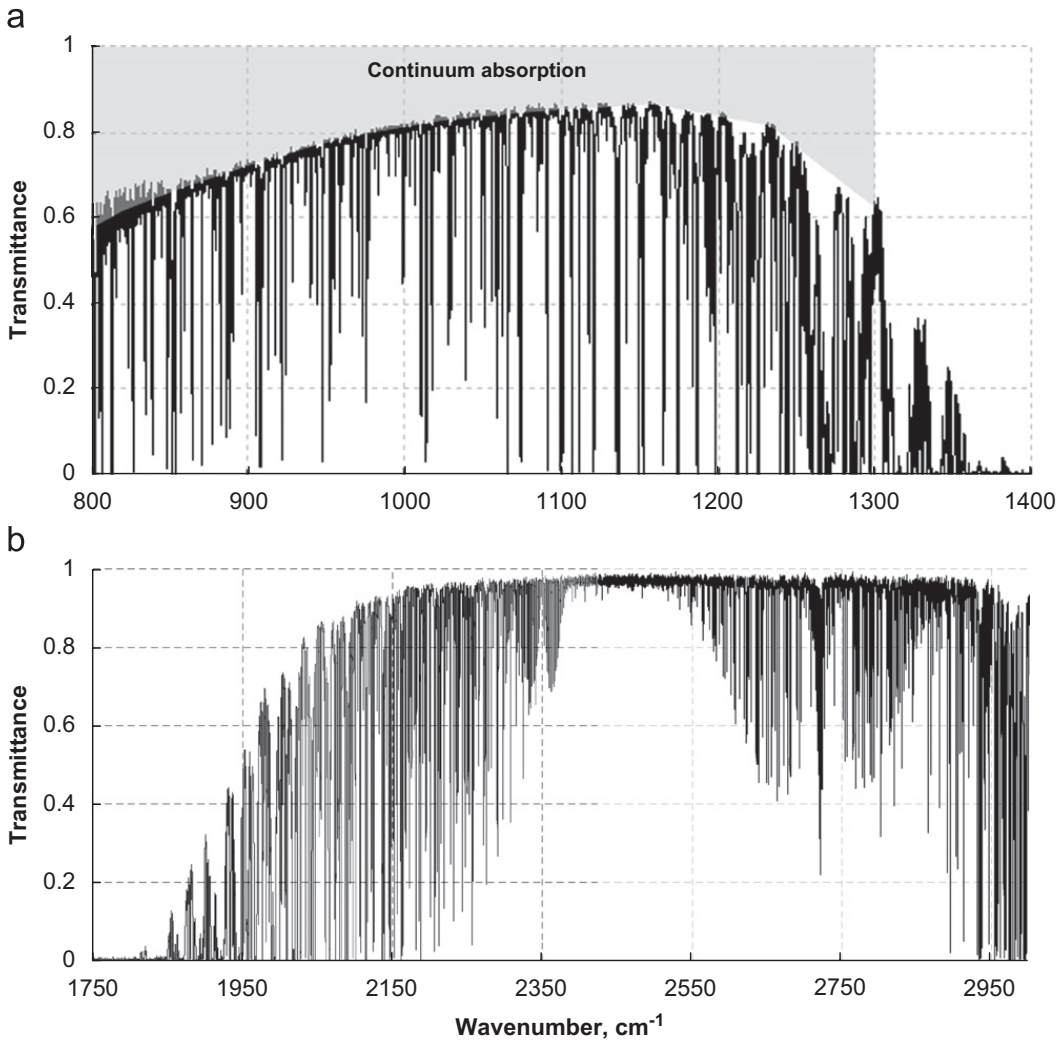

Fig. 1. Two segments of the infrared spectrum of pure water vapor recorded at 339.2 K with a path length of 92.05 m. The water-vapor pressure is 119.3 mbar (89.5 Torr). The continuum absorption in the lower frequency region is indicated.

extended theoretical study is required. We do not provide here a detailed overview of the continuum research since the most recent papers by Tobin et al. [4] and Cormier et al. [5] contain quite large lists of references, reflecting the current status of the problem. We will just refer to the most important works dealing with laboratory continuum investigations under accurately defined conditions.

As it is shown in Fig. 1(a), the saturated water-vapor spectrum in the region of study consists of many ro-vibrational lines sitting on top of a concave-shaped pedestal, which is the water-vapor continuum. This continuous absorption is proportional to the square of the water-vapor density and can be considered as a collisional effect. Usually the water-vapor continuum absorption coefficient is written as [6]

$$k_{\mathrm{cont}}(\nu,\Theta) = -\ln\left(T_{\mathrm{cont}}(\nu,\Theta)\right)L^{-1} = C_{\mathrm{s}}(\nu,\Theta)\rho_{\mathrm{H_2O}}[P_{\mathrm{H_2O}} + \gamma(P - P_{\mathrm{H_2O}})] \quad (1)$$

where ν and Θ are the wavenumber and temperature, T_{cont} is a transmission coefficient, L is a path length in cm, $\rho_{\mathrm{H_2O}}$ is the vapor density in molec cm^{-3}, $P_{\mathrm{H_2O}}$ is the vapor partial pressure in atm, P is the total sample pressure, C_{s} is the self-broadened continuum binary absorption coefficient in cm^{-1}(molec/cm^3)$^{-1}$ atm^{-1} units[1],

[1]Note that the continuum MT_CKD software [7] gives absorption coefficients in cm^{-1}(molec/cm^3)$^{-1}$ units normalized to the standard atmosphere conditions used in HITRAN [8], i.e. 1 atm pressure at 296 K (1 atm = 760 Torr = 1013 mbar = 101.3 kPa). Therefore, the continuum binary absorption coefficients reported in cm^{-1}(molec/cm^3)$^{-1}$atm^{-1} at 296 K are equal to the MT_CKD values. But absorption coefficients reported in cm^{-1}(molec/cm^3)$^{-1}$atm^{-1} for temperature $\Theta \neq 296$ K must be converted by multiplying by the factor $\Theta/296$ K before comparing with the MT_CKD values.

and $\gamma = C_f/C_s$ is the ratio of the foreign-gas broadened absorption coefficient to the self-broadened coefficient. Since $\gamma << 1$ (see for example [5,6]), the self-broadened continuum absorption plays an important role when the humidity is high in the Earth's troposphere.

Both the wavenumber and temperature dependence of the continuum are critical for atmospheric applications. Burch and co-workers [9–11] initially carried out systematic and quantitative laboratory measurements of the water continuum as well as other weak absorptions of IR radiation by CO_2. They used two 30 and 1 m multipass cells with a grating spectrometer and provided continuum absorption coefficients over wide wavenumber ranges at several temperatures. In addition, McCoy et al. [12] and later Nordstrom et al. [13] measured the water-vapor continuum absorption at room temperature using a 15.5 m base White cell and a tunable CO_2 laser as a radiation source. The results for several laser transitions were reported. A 50 m base multipass cell and a tunable CO_2 laser have been used by Aref'ev and co-workers to measure water-vapor absorption at room and elevated temperatures, and an empirical water-vapor continuum model was developed on the basis of these investigations [14,15]. This model uses an exponential law for the continuum temperature dependence. Their exponent parameter is independent of the wavenumber and derived from measurements at the 10P(20) (944.19 cm^{-1}) laser transition. In 1979 Peterson et al. [16] reported continuum measurements with a tunable CO_2 laser and multipass cells. Experiments were carried out at room temperature over the 935–1082 cm^{-1} spectral range. Later a spectrophone technique with a tunable CO_2 laser was used to study the continuum absorption at different temperatures between 263 and 300 K [17] and 253–345 K [18]. The analysis of the observed temperature dependence led the authors [18] to the conclusion that it is exponential but not uniform for the three laser transitions used in the measurements. Finally we note several experiments attempting to measure the water-vapor continuum with shorter multipass cells with a base length of ~1–2 m. These experiments were carried out at elevated temperatures allowing higher water-vapor pressures, which make the continuum easily measurable at path lengths of several tens of meters [19–21]. Montgomery [19] has studied the continuum temperature dependence with a path length of 40 m using a diode laser operating at a fixed wavenumber of 1203 cm^{-1}. He observed that the absorption coefficient at temperatures between 333 and 473 K exhibit a parabolic temperature dependence with a minimum at 400 K. Recently a Cavity Ring-Down Spectroscopy method was used to explore the water-vapor continuum temperature dependence at the 10P(20) CO_2 laser transition (944.19 cm^{-1}) [5]. An exponential decrease of the absorption coefficient was found in the 276–310 K temperature range. Every experimental technique used for the continuum measurements has its own "pluses" and "minuses", which were considered by Grant [22]. However, a high-resolution spectrometer with a multipass cell is preferable since it provides data over a wide wavenumber range. Our conclusion from this overview is that there is an obvious scarcity of reliable data on the water-vapor continuum, both the wavenumber and temperature dependence, over the entire range of this atmospheric window. Only the data of Burch et al. [10,11] cover a wide spectral range. However, these data do not allow an accurate retrieval of the continuum wavenumber and temperature dependence because they were measured at just three temperatures, and with a comparatively low resolution of 0.3 cm^{-1}. The possibilities for computational data processing were limited at that time. The other data are not equal in accuracy and provide only limited information about the continuum wavenumber and temperature dependence. Nevertheless, the most reliable and accurate data were selected and used by Clough and co-workers to develop the well-known CKD continuum models [1], widely used in atmospheric radiative transfer calculations. Recent progress in spectroscopic and computational techniques allow us to take the next step in laboratory measurements of the continuum in order to obtain more accurate data for atmospheric applications, and to aid in our understanding of the physical mechanisms responsible for the continuum over a wider range of temperatures.

2. Experimental

The NIST experimental setup for the spectroscopic investigation of gases has been described previously [4]. We focus here only on the specific details regarding measuring the infrared absorption of pure water vapor. The system consists of a BOMEM DA3-002 FTIR spectrometer[2] with a 2 m base White-type multi-pass cell.

[2]Certain commercial equipment instruments or materials are identified in this paper to adequately specify the experimental procedure. Such identification does not imply recommendation or endorsement by the National Institute of Standards and Technology, nor does it imply that the materials or equipment identified are necessarily the best available for the purpose.

This cell is equipped with all the equipment (pumps, pressure gauges, thermo-controller, etc.) necessary to operate with gases in the temperature range from −90 °C to +90 °C and with pressures up to 8 atm (depending on the choice of windows). Path lengths of up to 116 m can be obtained.

A simple estimate based on available values of absorption coefficients C_s shows that a path of 116 m is too short for accurate measurements of the continuum at room temperature, where the maximum vapor pressure of water is about 26 mbar. However, this path length will be quite adequate for measurements at slightly elevated temperatures where pressures of several tens of Torr can be obtained because the continuum absorption increases as the square of the water-vapor density (see Eq. (1)). The only technical problem is to obtain a uniform temperature over all the internal surfaces of the cell body and to avoid vapor condensation. Every multi-pass cell has some protruding parts such as the inlet and outlet valves, window holders, sleeves, etc. that may have significantly lower temperatures than that of the cell body. In order to obtain a uniform temperature, all these parts were equipped with additional electric heaters and coated with thermo-insulation. We have also installed several additional thermocouples to measure and control the temperature of these parts.

A Barocell 600A type (133 mbar range) pressure gauge connected directly to the cell flange was used for the water-vapor pressure measurements. The gauge body was also heated with an additional electric heater. Assuming that the gauge properties would change with temperature, we performed periodic calibrations filling the cell with nitrogen and measuring the pressure with a second gauge (MKS, Baratron 270, 1333 mbar) operating at room temperature. The calibration signal-pressure dependence was found to be linear and stable. The estimated type B relative standard uncertainty of measured pressure is about 0.6%.

A simple device was specially designed to fill the cell with water vapor. It is a brass cylindrical vessel with a volume of about 400 cm^3 and internal diameter of about 5 cm. The cylinder is horizontally positioned and equipped with an inlet cap to fill it with distilled water. The horizontal position provides a maximized water surface and rate of evaporation. An electric heater and thermal insulation were also installed. The liquid water temperature was kept close to that of the cell body. Fifteen to 30 min were used to fill the cell with water vapor in order to maintain thermal equilibration and to maintain the stability of the cell optics.

Three standard copper/constantan thermocouples installed inside the cell, one in the center and two near the flanges, were used for temperature measurements. The difference between temperatures was not greater than 0.3 K.

The instrumental spectral resolution was set at 0.1 cm^{-1}. This value was chosen to take into account two opposing circumstances. It is well known that MCT detector nonlinearity may lead to systematic errors in the measured transmittance. To minimize this error, it is necessary to reduce the beam's radiance by setting the instrument's aperture to a minimum size. At this radiance level an acceptable signal-to-noise ratio can be obtained after about 300 scans. A reasonable time for one experiment is about 2 or 3 h. There are two things that limit the measurement time. While recording spectra, we noticed every time that the water-vapor pressure dropped slightly typically about 0.2% per hour. This process is linear within 1 or 2 h. We assumed that this is a result of molecular adsorption on the surfaces within the cell and/or vapor condensation in the micro-gaps of the cell construction. In addition, there is a base line drift due to instrumental limitations. The resolution chosen then is a compromise, which produces an acceptable signal-to-noise ratio within about 3 h.

Each experiment consists of several stages. Initially, a base line is recorded while the cell was being pumped. The cell is then filled with water vapor and allowed to equilibrate for about 10 min. For the effective pressure, we take the average of the values at the beginning and end of the sample scan. At the finish of the sample scan, the cell is pumped out, and a second base line spectrum was recorded. The end product in transmittance units is the ratio of the water vapor spectrum to the average of the base line spectra. A summary of the experimental conditions is given in Table 1.

All spectra were recorded over the 780–3500 cm^{-1} spectral region, which covers both mid-infrared atmospheric windows. The low-frequency limit is caused by the cutoff of the BaF_2 windows. At wavenumber above 3500 cm^{-1}, the water absorption is saturated over a wide range. A sample spectrum is shown in Fig. 1. In the low-frequency segment of the spectrum (a), an easily measurable continuum is observed. Its absorbance of about 20% is shown in light gray. In the regions where the individual lines are completely absorbing, the transmittance is in excellent agreement with the zero of the transmittance scale, which indicates that there are no distortions of the zero level resulting from detector nonlinearity. Note that there is a trace of

Table 1
Experimental conditions and number of spectra recorded at different temperatures

Temperature (K) (±0.3 K)	Pressure range (mbar) (Torr)	Path length (m)	Number of spectra recorded
310.8	28.3–60.6 (21.2–45.5)	68–116	41
318.0	34.0–74.2 (25.5–55.7)	84–116	46
325.8	44.9–115 (33.7–86.3)	76–116	48
339.3	52.1–123 (39.1–92.0)	84–108	51
351.9	57.6–151 (43.2–113)	84–116	51
363.6	54.8–137 (41.1–103)	84–116	36

the CO_2 v_3 fundamental band at 2346 cm^{-1} observed in the spectrum. We estimate that the typical amount of CO_2 present is about 1 ppmv. Even when doubly distilled water was used, this band was evident in the spectra. We feel that this trace amount of CO_2 will have a negligible effect on the H_2O continuum. No other impurities were seen in the spectra. We also note that weak continuous absorption is detected in the high-frequency window of the spectra. The analysis of this absorption will be dealt with in a future paper. This absorption is not due to base line error. Many tests of the base line stability using N_2 up to 3 atm prove that only random variations of the baseline within 0.3% were measured. The baseline scatter has been found to be temperature independent.

3. Data processing

The quickest and simplest method to obtain the continuum binary absorption coefficients is to measure directly the transmittance in the micro-windows between the ro-vibrational lines. Our calculations based on the HITRAN04 database [8] show that there are quite a number of micro-windows in the range 800–1150 cm^{-1} where the contribution of the local lines to the absorption is negligible. Fig. 2 displays a few spectra obtained in a micro-window around 943 cm^{-1} together with a calculated spectrum for the highest pressure. This spectrum demonstrates negligible absorbance in the segment inside of the frame. Therefore the measured transmittances over this segment can be used for direct retrieval of the continuum binary absorption coefficient C_s. In Fig. 3, we have plotted all the measured absorbances against the square of the vapor density for two temperatures. The NIST Chemistry Webbook [23] (www.webbook.nist.gov/chemistry/), which corrects for non-ideal gas behavior, was used to convert the measured values of the water-vapor pressure to density. The plots are quite linear. The slopes of these plots are the binary absorption coefficients C_s in cm^{-1} $(cm^3/molec)^2 \times 10^{-38}$ units.

Binary absorption coefficients have been determined for 27 micro-windows over the region from 800 to 1150 cm^{-1}. Because in these micro-windows local line contributions are negligible, one does not have to worry about effects from different definitions of the continuum adopted by different people. As a result, one can simply assume that the measured absorptions are equal to the continuum, and one can compare the experimental values with those of the MT_CKD model [7] directly. However, this is not true for other frequencies of interest.

The measured continuum binary absorption coefficients at six temperatures are listed in Table 2 as well as their type A standard uncertainties (one standard deviation). We believe that the type B systematic error caused by uncertainties in pressure and temperature does not exceed 2%. The same data are plotted in Fig. 4 together with values computed using the MT_CKD program [7]. Our theoretical results are also presented here. Fig. 4 indicates that the discrepancy between observed and predicted values by the MT_CKD model grows dramatically with temperature, reaching 50% for low frequency data. This leads us to the conclusion that the widely used MT_CKD model requires refinements. In contrast, the far-wing theoretical calculations provide a quite good agreement with the experimental data for wavenumbers lower than 870 cm^{-1}. At higher frequencies where the continuum absorptions are very weak, the agreement is not as good, but becomes better as the temperature increases.

At wavenumbers higher than 1150 cm^{-1}, the local line contribution becomes significant and the method used here is not adequate to retrieve the water vapor continuum absorption coefficients. Therefore we have

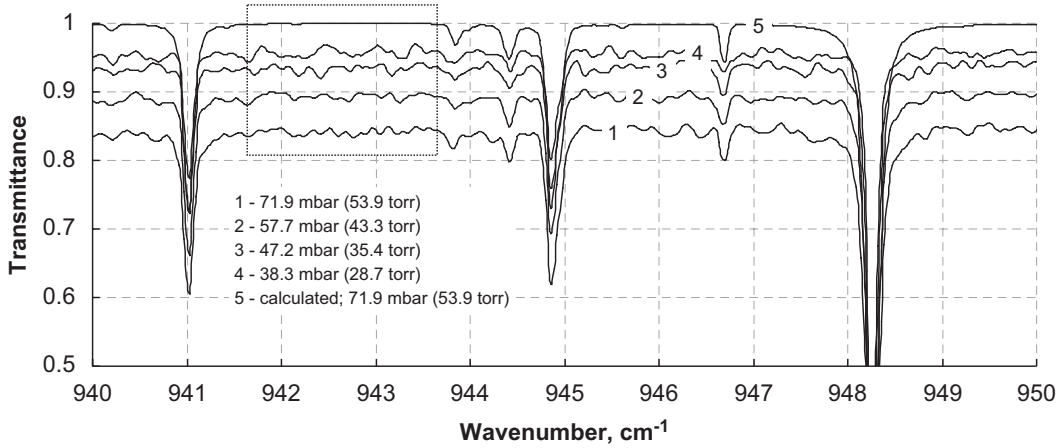

Fig. 2. A small portion of four spectra recorded at different pressures at a temperature of 318 K with a path length of 108 m. The upper curve shows the spectrum calculated for the highest pressure of 71.9 mbar (53.9 Torr) using the HITRAN04 database.

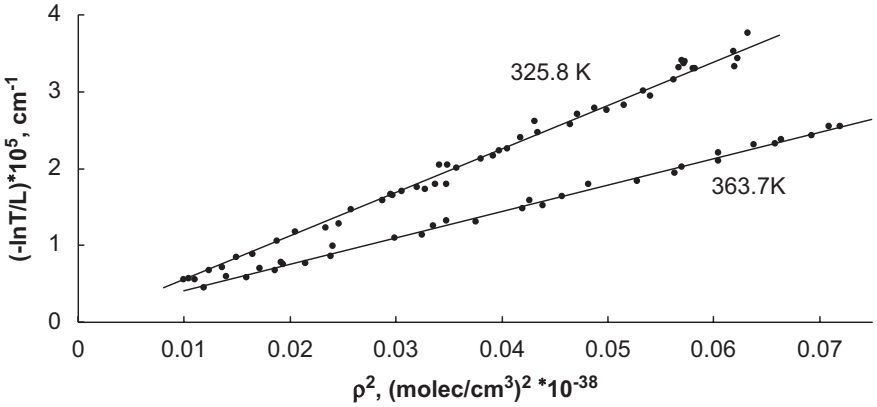

Fig. 3. Absorbance of the 943 cm^{-1} micro-window plotted versus the square of the vapor density at two temperatures.

developed an additional method to obtain the binary absorption coefficients over a broader range making use of the HITRAN database [8] to calculate and remove the ro-vibrational structure from the observed spectra. The calculation procedure is similar to that described recently in [24]. An observed spectrum in transmittance scale is represented as the product of two terms:

$$T_{\text{obs}}(\nu,\Theta) = T_{\text{cont}}(\nu,\Theta)\, T_{\text{struct}}(\nu,\Theta) \tag{2}$$

$$T_{\text{struct}}(\nu,\Theta) = \int_{\delta\nu} f(\nu-\nu')\, T_{\text{lin}}(\nu',\Theta)\, \mathrm{d}\nu' \tag{3}$$

where $T_{\text{cont}}(\nu,\Theta)$ is the transmittance of the water-vapor continuum, $T_{\text{lin}}(\nu,\Theta)$ the selective monochromatic transmittance, $f(\nu-\nu')$ a Gaussian instrumental function determined by fitting of the experimentally observed line profiles at low pressures. A selective monochromatic transmittance $T_{\text{lin}}(\nu,\Theta)$ is expressed as

$$T_{\text{lin}}(\nu,\Theta) = \exp\left(-PL\sum_i \frac{S_i(\Theta)}{\pi}\left(\frac{\gamma_i(P,\Theta)}{(\nu-\nu_i)^2+\gamma_i^2(P,\Theta)} - \frac{\gamma_i(P,\Theta)}{(25-\nu_i)^2+\gamma_i^2(P,\Theta)}\right)\right) \tag{4}$$

Here Θ and P are the water-vapor temperature and pressure, L is a path length, S_i, γ_i, and ν_i are the line intensity, half-width, and position for a given H_2O transition, respectively. For these calculations, we assumed a temperature coefficient for the half-widths of 0.745. The sum is taken over all of the lines in a spectral region of $\nu \pm 25\,cm^{-1}$. The second term in the internal brackets of Eq. (4) removes a line shape value at 25 cm^{-1} from a center, the so-called basement. Therefore this equation corresponds to the adopted continuum definition in

Table 2
Binary absorption coefficients of the water-vapor continuum derived by direct measurements of absorption in selected microwindows

310.8 K			318 K		325.8 K		339.3 K		351.9 K		363.6 K	
v (cm^{-1})	C_s	STDV	C_s	STDV	C_s	STDV	C_s	STDV	C_s	STDV	C_s	STDV
818.0	3.15	0.20	2.76	0.07	2.45	0.04	1.97	0.06	1.82	0.03	1.60	0.04
820.0	3.22	0.20	2.69	0.08	2.43	0.03	2.02	0.04	1.83	0.02	1.53	0.03
822.0	3.01	0.16	2.79	0.08	2.42	0.04	1.95	0.04	1.78	0.03	1.52	0.02
831.8	2.81	0.15	2.55	0.05	2.28	0.03	1.88	0.03	1.65	0.03	1.43	0.02
837.0	2.73	0.15	2.50	0.06	2.24	0.02	1.84	0.03	1.62	0.03	1.40	0.02
847.4	2.76	0.11	2.44	0.05	2.16	0.02	1.81	0.03	1.56	0.02	1.34	0.02
861.8	2.46	0.11	2.36	0.05	2.04	0.03	1.70	0.02	1.46	0.02	1.26	0.02
868.2	2.35	0.09	2.21	0.05	1.98	0.03	1.63	0.02	1.43	0.02	1.21	0.02
873.7	2.35	0.09	2.15	0.05	2.03	0.03	1.58	0.02	1.37	0.02	1.18	0.02
874.9	2.29	0.10	2.17	0.05	1.92	0.03	1.58	0.03	1.36	0.02	1.15	0.02
877.1	2.32	0.10	2.13	0.06	1.91	0.02	1.55	0.03	1.37	0.02	1.18	0.01
885.6	2.21	0.11	2.08	0.05	1.83	0.02	1.54	0.02	1.32	0.02	1.12	0.01
894.0	2.14	0.10	2.03	0.04	1.77	0.02	1.45	0.02	1.25	0.01	1.06	0.01
901.6	2.13	0.10	1.95	0.04	1.72	0.02	1.41	0.02	1.20	0.02	1.03	0.02
915.9	2.05	0.08	1.85	0.04	1.62	0.02	1.30	0.02	1.14	0.01	0.96	0.01
931.3	1.83	0.08	1.77	0.04	1.51	0.02	1.23	0.02	1.07	0.01	0.90	0.01
934.3	1.83	0.08	1.71	0.04	1.48	0.02	1.20	0.02	1.02	0.01	0.87	0.01
951.0	1.65	0.07	1.54	0.04	1.36	0.02	1.10	0.02	0.92	0.01	0.78	0.01
964.5	1.60	0.06	1.46	0.04	1.27	0.02	1.03	0.02	0.86	0.01	0.74	0.01
986.3	1.46	0.07	1.28	0.04	1.15	0.02	0.92	0.01	0.77	0.01	0.65	0.01
1023.7	1.21	0.05	1.13	0.04	0.98	0.02	0.79	0.02	0.66	0.01	0.58	0.01
1034.5	1.17	0.07	1.08	0.04	0.94	0.02	0.77	0.02	0.65	0.01	0.55	0.01
1046.0	1.11	0.08	1.03	0.03	0.91	0.02	0.77	0.02	0.60	0.01	0.54	0.01
1069.7	1.06	0.08	0.97	0.04	0.84	0.02	0.70	0.02	0.58	0.01	0.50	0.01
1095.5	0.96	0.07	0.95	0.04	0.79	0.02	0.67	0.02	0.55	0.01	0.48	0.01
1127.9	0.94	0.07	0.85	0.04	0.75	0.02	0.64	0.01	0.53	0.01	0.48	0.01
1144.5	0.94	0.06	0.84	0.03	0.74	0.02	0.63	0.02	0.53	0.02	0.49	0.01

Absorption coefficients and standard deviations in $cm^{-1}(molec/cm^3)^{-1}$ are multiplied by 1e + 22.

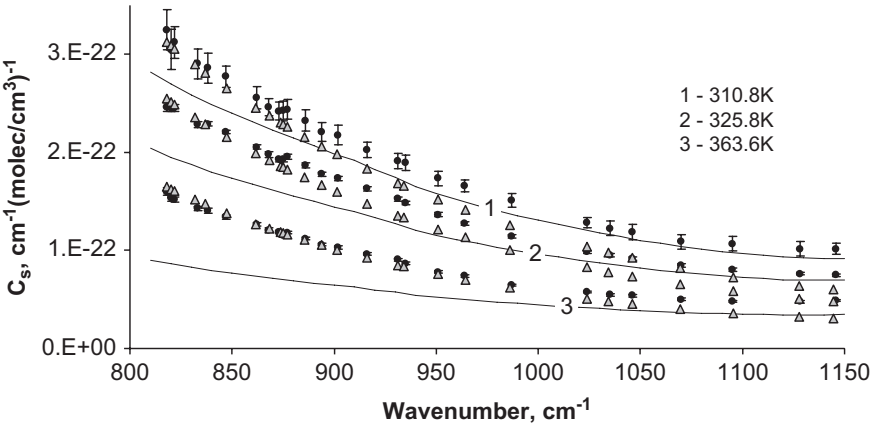

Fig. 4. Experimentally determined water continuum binary absorption coefficients are denoted by ● and the error bars are one standard deviation determined from a least squares fit. The theoretical values are denoted by Δ, and the MT_CKD values are given by solid lines. The three temperatures are numbered from the top to the bottom.

Ref. [1]. Fig. 5 represents an example of spectra after removal of the ro-vibrational structure. There are numerous spikes, which became stronger at higher pressures and temperatures. Note that in order to limit these distortions we omitted all spectral points of the original spectra where $T_{struct}(v,\Theta) \leqslant 0.3$. There are several sources that cause these spikes such as line parameter uncertainties, failure to take into account self-induced

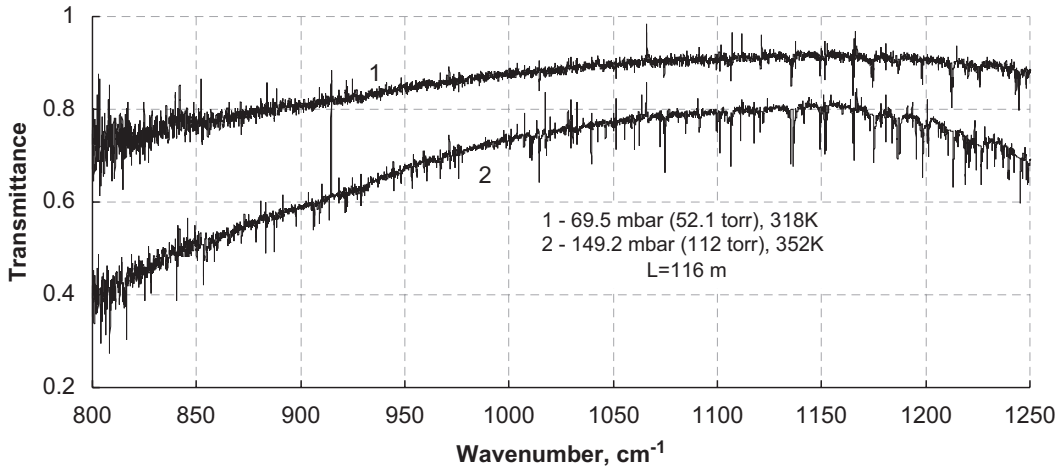

Fig. 5. Two water-vapor continuum spectra after removal of the ro-vibrational structure calculated with the HITRAN04 dataset and Lorentzian profiles.

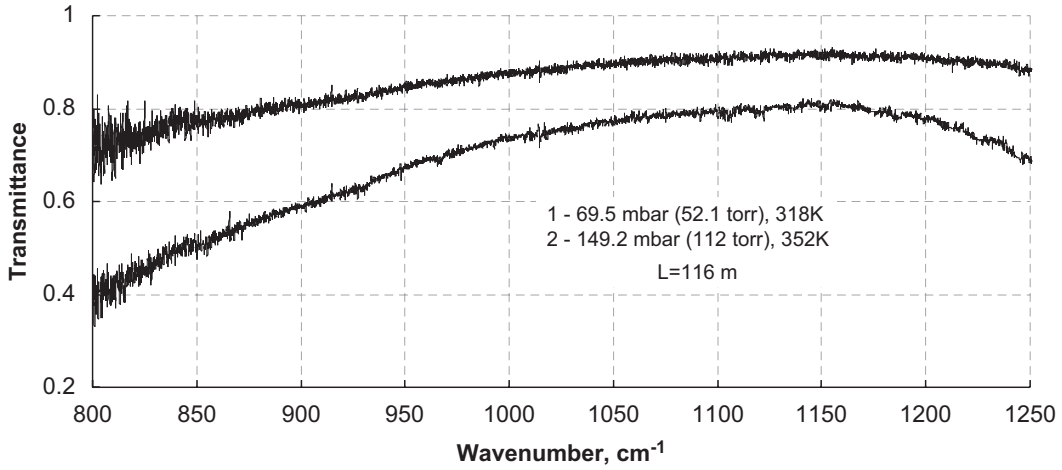

Fig. 6. The same two spectra after application of the modified program.

line shifting, the deviation of real line profiles from a Lorenz function because of line mixing [25], etc. A detailed analysis of this problem is beyond the scope of this paper. To solve the problem, we modified the program adding routines that fit the calculated ro-vibrational structure to that observed by varying the line parameters. Fig. 6 shows the same two spectra after applying this modified procedure.

All of the recorded spectra have been processed using this method, and used for the determination of the continuum binary absorption coefficients $b(\nu_k)$ at a given temperature by least squares fitting to the function:

$$-\ln\left(T_j(\nu_k)\right)L^{-1} = a(\nu_k) + b(\nu_k)\rho_j^2 \tag{5}$$

The subscript "j" denotes different spectra and corresponding gas densities ρ, and the subscript "k" denotes the different frequencies of the spectrum. The constant term $a(\nu_k)$ is included into Eq. (5) in order to compensate for possible minor systematic errors in the base line. After the binary coefficients were calculated, they were smoothed over a $4\,\mathrm{cm}^{-1}$ interval. The final set of our data on the water vapor continuum absorption coefficients[3] is shown in Fig. 7.

[3]The digital file is available from the authors.

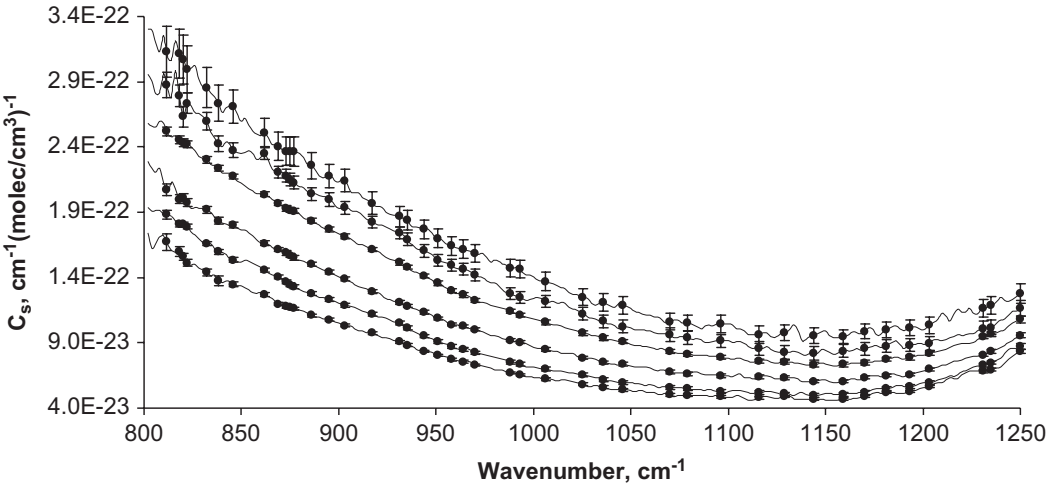

Fig. 7. The water-vapor continuum absorption coefficients at six temperatures: 310.8, 318.0, 325.8, 339.3, 351.9, and 363.6 K from the top to the bottom. The lines represent the continuum as a continuous function of wavenumber. The points represent the values at centers of relatively wide micro-windows with statistically estimated errors.

4. Analysis and discussion

Fig. 7 indicates that the smoothed continuum curves exhibit severe small bumps and fringes especially at the two lowest temperatures. Some of these features seem reproducible but, at present, we are not sure whether this is an instrumental artifact or a small problem with the data processing. Unfortunately the errors for the two lower temperatures are enhanced by the limitation on the water-vapor pressure. In addition, the signal-to-noise ratio drops rapidly for wavenumbers lower than 850 cm^{-1} because of the cut-off of the windows. We plan in the future to extend the wavenumber region down to 600 cm^{-1} by replacing the windows. Fig. 4 serves to emphasize the need for the temperature dependence of the water continuum to be explored thoroughly since the difference between the measurements of this study and the MT_CKD model grow dramatically at higher temperatures. Fig. 8 shows the temperature dependence of the continuum absorption coefficient at 944.19 cm^{-1}, which corresponds to the 10P(20) transition of the CO_2 laser. This transition is the strongest of the CO_2 laser lines and has been used by several investigators to measure the absorption coefficient at different temperatures. The figure shows the scarcity of data at temperatures lower than 296 K. It also indicates the need to check the data of Cormier et al. [5] since they differ significantly from all the other available data. The other measured values at 296 K are scattered between 2.02×10^{-22} $cm^{-1}/(molec/cm^3)$ (Peterson [16]) and 2.39×10^{-22} $cm^{-1}/(molec/cm^3)$ (Burch [11]). The value measured by Cormier et al. [5] is $1.82\pm0.02\times10^{22}$ $cm^{-1}/(molec/cm^3)$ and is considerably lower than these two previous works. We are led to the conclusion that the uncertainties cited in this work are very optimistic. It is interesting to note that the value of our coefficient extrapolated to 296 K is 2.2×10^{22} $cm^{-1}/(molec/cm^3)$, falling in the middle of the Peterson and Burch values, although the uncertainty of this estimate is rather large. Our measurements are in good agreement with those of Hinderling et al. [18] in the temperature region where the data overlap.

Fig. 9 shows a similar plot giving the continuum temperature dependence at 1203 cm^{-1}. Although the uncertainties in the values of the absorption coefficients obtained by Montgomery et al. [19] are relatively high, they indicate that the absorption coefficients increase at temperatures higher than 400 K. Our data combined with data of Burch [11] also indicate there is an increase in the absorption coefficients at the higher temperatures. This contradicts the MT_CKD predictions. However, measurements at more elevated temperatures will be required to prove this conclusively.

There are two theories regarding the dominant mechanism of the water-vapor continuum. Ma and Tipping [26,27] propose that it arises from the cumulative absorption of the far wings of strong lines of pure rotational transitions as well as those from the v_2 band. It is seen from Fig. 4 that the theoretical results fall below the experimental data at wavenumbers higher 900 cm^{-1}; however, the theory provides reasonable agreement with the strong negative temperature dependence of the continuum.

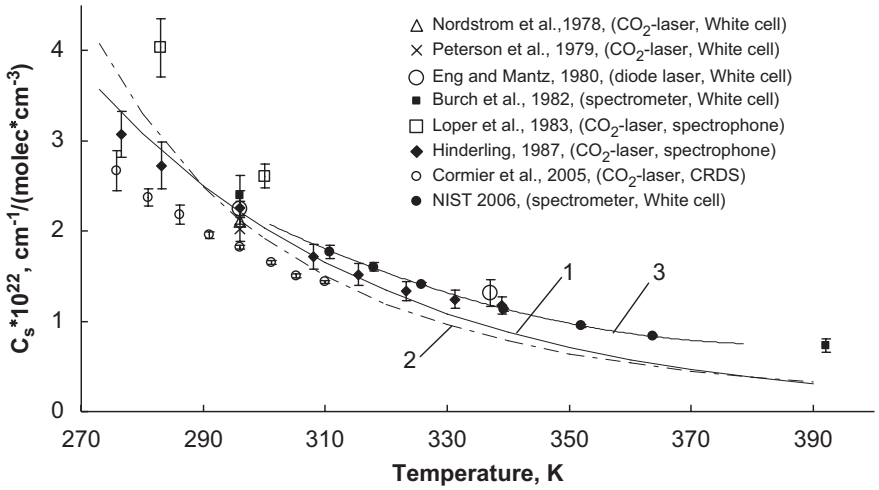

Fig. 8. The 944.19 cm^{-1} water-vapor continuum absorption coefficient at different temperatures in which the values obtained by several laboratories are compared. The solid line (1) was calculated using the MT_CKD continuum model, while the dashed line (2) was obtained using the continuum model developed by Aref'ev [14]. The line labeled (3) is a fitting of our measured data to a second-degree polynomial.

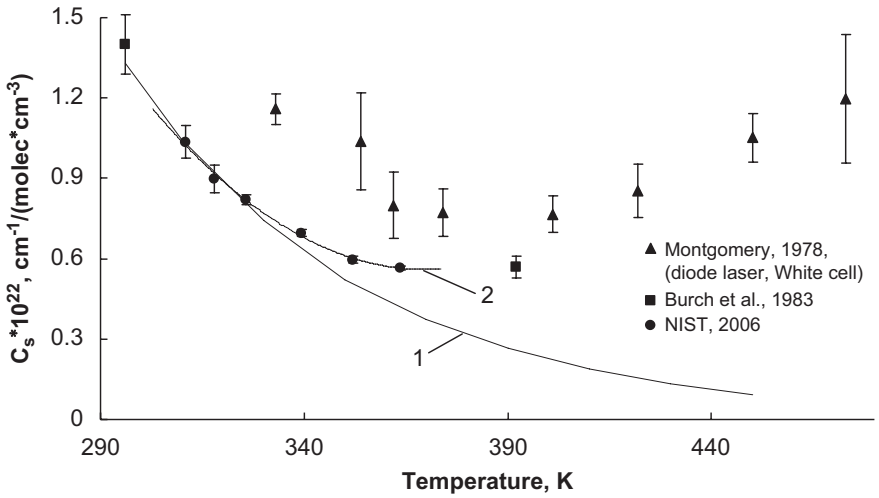

Fig. 9. The water-vapor continuum absorption coefficient at 1203 cm^{-1} over the temperature range 290–480 K. The line (1) shows the values calculated by the MT_CKD program, while line (2) is a fitting of our measured data to a second-degree polynomial.

On the other hand, there are reliable thermodynamic grounds to assume the presence of significant amounts of water-vapor dimers [28]. This assumption provides a very clear understanding of the temperature dependence of the continuum absorption. Almost all previous measurements of the temperature dependence obtained with different techniques for this spectral region lead to similar results in that the continuum absorption decreases exponentially with increasing temperature, and the rate of decrease is in good agreement with the independently derived dissociation energy of the water dimer [14,18,29,30]. Vigasin [31] has proposed a theoretical approach for the dimer absorption where the T-dependence is not purely exponential. This model was applied to recent measurements of Cormier et al. [5]. The water dimer dissociation energy derived by fitting of experimental data has been found to be consistent with the theoretical prediction of Goldman et al. [28]. We have to emphasize here that the continuum temperature dependence is not uniform. Our results combined with data of Burch et al. [11] are plotted in Fig. 10 with typically used scales (natural logarithm versus the reciprocal of the temperature). The figure demonstrates strong changes of the continuum T-dependence with wavenumber. It is exponential only in the lower-frequency part of the window. At wavenumbers higher than 1000 cm^{-1}, the continuum temperature dependence is not exponential, especially at higher temperatures, where it becomes rather parabolic, in contrast to results mentioned above. Recently,

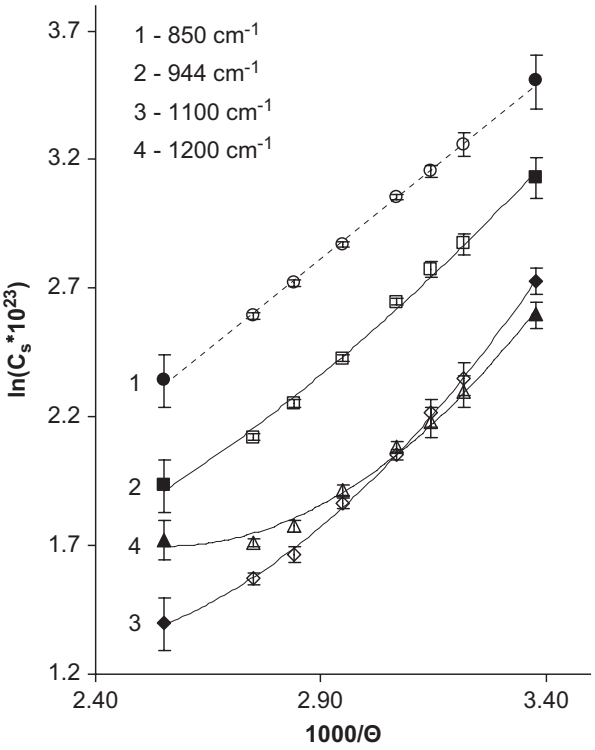

Fig. 10. A plot of the natural log of the binary absorption coefficient $\times 10^{23}$ of the water-vapor continuum versus the reciprocal of the temperature times 1000. Solid figures represent data of Burch et al. [9].

theoretical calculations by Scribano and Leforestier [32] showed that for wavenumbers between 20 and 500 cm^{-1}, the water dimers play only a minor role, but it is still an open question, whether dimers contribute significantly in other spectral regions. Another possible water vapor continuum mechanism was proposed by Bauer and Godon [33] for the millimeter spectral region. They suggested that there may be a significant collision-induced absorption (CIA) contribution to the water continuum in this region. For higher wavenumber regions, the first theoretical calculation of CIA in water vapor–nitrogen mixtures [34] showed that the calculated CIA absorption was found to be at least two orders smaller than the measured values in the 300–2000 cm^{-1} region. At present, we can conclude that the origin of the continuum is still not completely understood, and possibly all three mechanisms play a role in its formation in various spectral regions.

Acknowledgments

The authors would like to acknowledge Dr. S. A. Clough and Dr. J.-M. Flaud for their interest in this work and helpful discussions. We are also indebted to Dr. J.T. Hodges for his suggestions on this manuscript. The authors from NIST acknowledge with thanks support from the Upper Atmospheric Research Program of NASA. Ma and Tipping acknowledge financial support from NASA under Grants NAG5-13337, NNG06GB23G, and FCCS-547.

References

[1] Clough SA, Kneizys FX, Davies RW. Line shape and the water vapor continuum. Atmos Res 1989;23:229–41.
[2] Clough SA, Iacono MJ, Moncet J-L. Line-by-line calculation of atmospheric fluxes and cooling rates: application to water vapor. J Geophys Res 1992;97:15,761–85.
[3] Elsasser WM. Heat transfer by infrared radiation in the atmosphere. Harvard Meteorological Society. Cambridge (MA): Harvard University Press; 1942.

[4] Tobin DC, Strow LL, Lafferty WJ, Olson WB. Experimental investigation of the self- and N_2-broadened continuum within the v_2 band of water vapor. Appl Opt 1996;35:4724–34.
[5] Cormier JG, Hodges JT, Drummond JR. Infrared water vapor continuum absorption at atmospheric temperatures. J Chem Phys 2005;122:114309.
[6] Roberts RE, Selby JE, Biberman LM. Infrared continuum absorption by atmospheric water vapor in the 8–12-μm window. Appl Opt 1976;15:2085–90.
[7] Clough SA, Shephard MW, Mlawer EJ, Delamere JS, Iacono MJ, Cady-Pereira K, et al. Atmospheric radiative transfer modeling: a summary of the AER codes. JQSRT 2005;91:233–44 (see 〈www.aer.com〉).
[8] Rothman LS, Jacquemart D, Barbe A, Benner DC, Birk M, Brown LR, et al. The HITRAN 2004 molecular spectroscopic database. JQSRT 2005;96:139–204.
[9] Burch DE, Gryvnak DA, Patty RR. Absorption of infrared radiation by CO_2 and H_2O. Experimental techniques. J Opt Soc Am 1967;57:885–95.
[10] Burch DE, Gryvnak DA. Continuum absorption by H_2O vapor in the infrared and millimeter wave regions. In: Deepak A, Wilkerson TD, Ruhnke LH, editors. Atmospheric water vapor. New York: Academic Press; 1980. p. 47–76.
[11] Burch DE. Continuum absorption by H_2O. Technical report AFGL-TR-81-0300. Air Force Geophysical Laboratory, 1982.
[12] McCoy JH, Rensch DB, Long RK. Water vapor continuum absorption of carbon dioxide laser radiation near 10 μ. Appl Opt 1969;8: 1471–7.
[13] Nordstrom RJ, Thomas ME, Peterson JC, Damon EK, Long RK. Effects of oxygen addition on pressure-broadened water vapor absorption in the 10-μm region. Appl Opt 1978;17:2724–9.
[14] Dianov-Klokov VI, Ivanov VM, Aref'ev VN, Sizov NI. Water vapor continuum absorption at 8–13 μ. JQSRT 1981;25:83–92.
[15] Aref'ev VN. Molecular water vapor absorption of radiation in the 8–13 μm atmospheric relative transparency window. Atmos Ocean Opt 1989;2(10):878–94.
[16] Peterson JC, Thomas ME, Nordstrom RJ, Damon EK, Long RK. Water vapor-nitrogen absorption at CO_2 laser frequencies. Appl Opt 1979;18:834–41.
[17] Loper GL, O'Neill MA, Gelbwachs JA. Water-vapor continuum CO_2 laser absorption spectra between 27 °C and −10 °C. Appl Opt 1983;22:3701–10.
[18] Hinderling J, Sigrist MW, Kneubuhl FK. Laser-photoacoustic spectroscopy of water-vapor continuum and line absorption in the 8–14 μm atmospheric window. Infrared Phys 1987;27:63–120.
[19] Montgomery Jr GP. Temperature dependence of infrared absorption by the water vapor continuum near 1200 cm^{-1}. Appl Opt 1978; 17:2299–303.
[20] Varanasi P, Chudamani S. Self- and N_2-broadened spectra of water vapor between 7.5 and 14.5 μm. JQSRT 1987;38:407–12.
[21] Eng RS, Mantz AW. Tunable diode laser measurements of water vapor continuum and water vapor absorption line shape in the 10 μm atmospheric transmission window region. In: Deepak A, Wilkerson TD, Ruhnke LH, editors. Atmospheric water vapor. New York: Academic Press; 1980. p. 101–11.
[22] Grant WB. Water vapor absorption coefficients in the 8–13-μm spectral region: a critical review. Appl Opt 1990;29:451–62.
[23] NIST Chemistry WEB BOOK at 〈www.webbook.nist.gov/chemistry/〉.
[24] Baranov YI, Lafferty WJ, Fraser GT. Infrared spectrum of the continuum and dimer absorption in the vicinity of the 0–2 vibrational fundamental of O_2/CO_2 mixtures. J Mol Spectrosc 2004;228:432–40.
[25] Brown LR, Benner DC, Devi VM, Smith MAH, Toth RA. Line mixing in self- and foreign-broadened water vapor at 6 μm. J Mol Struct 2005;742:111–22.
[26] Tipping RH, Ma Q. Theory of the water vapor continuum and validations. Atmos Res 1995;36:69–94.
[27] Ma Q, Tipping RH. The averaged density matrix in the coordinate representation: application to the calculation of the far-wing line shapes for H_2O. J Chem Phys 1999;111:5909–21;
The density matrix of H_2O-N_2 in the coordinate representation: a Monte Carlo calculation of the far-wing line shape. J Chem Phys 2000;112:574–84;
The frequency detuning correction and the asymmetry of line shapes: the far wings of H_2O-H_2O. J Chem Phys 2002;116:4102–15.
[28] Goldman N, Leforestier C, Saykally RJ. Water dimers in the atmosphere II: results from the VRT(ASP-W)III potential surface. J Phys Chem 2004;A108:787.
[29] Varanasi P. On the nature of the infrared spectrum of water vapor between 8 and 14 μm. JQSRT 1988;40:169–75.
[30] Paynter DJ, Ptashnik IV, Shine KP, Smith KM. Pure water vapor continuum measurements between 3100 and 4400 cm^{-1}: evidence for water dimer absorption in near atmospheric conditions. Geophys Res Lett 2007;34:L12808.
[31] Vigasin AA. Water vapor continuum absorption in various mixtures: possible role of weakly bound complexes. JQSRT 2000;64: 25–40.
[32] Scribano Y, Leforestier C. Contribution of water dimer absorption to the millimeter and far infrared atmospheric water continuum. J Chem Phys 2007;126:234301.
[33] Bauer A, Godon M. Continuum for H_2O-X mixtures in the H_2O spectral window at 239 GHz; $X = C_2H_4$, C_2H_6. Are collision induced absorption processes involved? JQSRT 2001;69:277–90.
[34] Brown A, Tipping RH. Collision-induced absorption in dipolar molecule–homonuclear diatomic pairs. In: Camy-Peyret C, Vigasin AA, editors. Weakly interacting molecular pairs: unconventional absorbers of radiation in the atmosphere. Netherlands: Kluwer Academic Publishers; 2003. p. 93–9.